# Metal−Ligand Interplay in Blue Copper Proteins Studied by ^{1}H NMR Spectroscopy: Cu(II)−Pseudoazurin and Cu(II)−Rusticyanin

Antonio Donaire,[†] Beatriz Jiménez,[§] Claudio O. Fernández,[#] Roberta Pierattelli,[×] Tomotake Niizeki,[⊥] José-María Moratal,[§] John F. Hall,[||] Takamitsu Kohzuma,[⊥] S. Samar Hasnain,[||,∇] and Alejandro J. Vila*,[‡]

*Contribution from the Biophysics Section and Instituto de Biología Molecular y Celular de Rosario (IBR), University of Rosario, Suipacha 531, S2002LRK Rosario, Argentina, Centro de Biología Molecular y Celular, Universidad Miguel Hernández, Edificio Torregaitán, Avda. Ferrocarril s/n, 03202-Elche (Alicante), Spain, Departamento de Química Inorgánica, Universitat de València, C/ Dr. Moliner, 50, 46100-Burjassot (Valencia), Spain, LANAIS RMN-300, University of Buenos Aires-CONICET, Junín 956, C1113AAD Buenos Aires, Argentina, Department of Chemistry and CERM, Via L. Sacconi, 6-50019 Sesto Fiorentino, Italy, Department of Chemistry, Faculty of Science, Ibaraki University, Mito, Ibaraki 310-8512, Japan, The Cell Signaling Laboratory, Department of Biological Sciences, De Monfort University, The Gateway, Leicester LE1 9BH, U.K., and CCLRC Daresbury Laboratory, Warrington, Cheshire WA4 4AD, U.K.*

Received April 26, 2002

*Abstract:* The blue copper proteins (BCPs), pseudoazurin from *Achromobacter cycloclastes* and rusticyanin from *Thiobacillus ferrooxidans,* have been investigated by ^{1}H NMR at a magnetic field of 18.8 T. Hyperfine shifts of the protons belonging to the coordinated ligands have been identified by exchange spectroscopy, including the indirect detection for those resonances that cannot be directly observed (the $\beta$-CH$_2$ of the Cys ligand, and the NH amide hydrogen bonded to the S$_\gamma$(Cys) atom). These data reveal that the Cu(II)−Cys interaction in pseudoazurin and rusticyanin is weakened compared to that in classic blue sites (plastocyanin and azurin). This weakening is not induced by a stronger interaction with the axial ligand, as found in stellacyanin, but might be determined by the protein folding around the metal site. The average chemical shift of the $\beta$-CH$_2$ Cys ligand in all BCPs can be correlated to geometric factors of the metal site (the Cu−S$_\gamma$(Cys) distance and the angle between the CuN$_{His}$N$_{His}$ plane and the Cu−S$_\gamma$(Cys) vector). It is concluded that the degree of tetragonal distortion is not necessarily related to the strength of the Cu(II)−S$_\gamma$(Cys) bond. The copper−His interaction is similar in all BCPs, even for the solvent-exposed His ligand. It is proposed that the copper *xy* magnetic axes in blue sites are determined by subtle geometrical differences, particularly the orientation of the His ligands. Finally, the observed chemical shifts for $\beta$-CH$_2$ Cys and Ser NH protons in rusticyanin suggest that a less negative charge at the sulfur atom could contribute to the high redox potential (680 mV) of this protein.

## Introduction

Blue copper proteins (BCPs) are electron-transfer mononuclear copper proteins distinguished by their unique spectroscopic features and high redox potentials compared to those of normal Cu(II) complexes.[1−6] The unusual spectroscopic proper-

ties of BCPs in the oxidized state, namely, an intense ligand-to-metal charge-transfer band in the visible absorption spectrum and a small $A_{||}$ hyperfine coupling constant in the EPR signal, have been attributed to the high covalence of the conserved Cu(II)−S$_\gamma$(Cys) moiety.[4,7] The coordination sphere of the copper ion in BCPs is completed by two histidine residues and a weaker, axial ligand interaction, which is a Met residue in most cases (Figure 1).

The high redox potentials of BCPs have been attributed to the soft−soft stabilizing interaction between the reduced copper

* Address correspondence to this author. Phone: +54-341-4350596. Fax: +54-341-4390465. E-mail: vila@arnet.com.ar/avila@fbioyf.unr.edu.ar.
‡ University of Rosario.
† Universidad Miguel Hernández.
§ Universitat de València.
# University of Buenos Aires-CONICET.
× University of Florence.
⊥ Ibaraki University.
|| De Monfort University.
∇ CCLRC Daresbury Laboratory.

(1) Adman, E. T. *Adv. Protein Chem.* **1991**, *42*, 144−197.
(2) Messerschmidt, A. *Struct. Bonding* **1998**, *90*, 37−68.
(3) Gray, H. B.; Winkler, J. R. *Annu. Rev. Biochem.* **1996**, *65*, 537−561.
(4) Randall, D. W.; Gamelin, D. R.; LaCroix, L. B.; Solomon, E. I. *J. Biol. Inorg. Chem.* **2000**, *5*, 16−19.
(5) Gray, H. B.; Malmström, B. G.; Williams, R. J. P. *J. Biol. Inorg. Chem.* **2000**, *5*, 551−559.
(6) Vila, A. J.; Fernandez, C. O. In *Handbook of Metalloproteins*; Bertini, I., Sigel, H., Eds.; Marcel Dekker: New York, 2001; pp 813−856.
(7) Shadle, S. E.; Penner-Hahn, J. E.; Schugar, H. J.; Hedman, B.; Hodgson, D. J.; Solomon, E. I. *J. Am. Chem. Soc.* **1993**, *115*, 767−776.
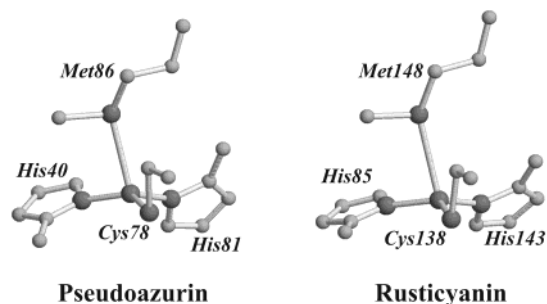
**Figure 1.** Schematic representation of the metal site in Cu(II)−pseudoazurin from *Achromobacter cycloclastes*, from the PDB file 1bqk,[40] and Cu(II)−rusticyanin from *Thiobacillus ferrooxidans*, from the PDB file 1rcy.[41]

ion and the $S_\gamma$(Cys) atom, and to the existence of a strained and destabilizing coordination for the copper(II) form.[5,8] It has also been suggested that the long Cu−S$_{Met}$ bond allied to the short Cu−S$_\gamma$(Cys) bond destabilizes the oxidized state more than the reduced state.[4,9] These ideas have been challenged recently, since the redox potential of a partially unfolded azurin possesses a higher redox potential than the protein in its native conformation; i.e., the protein folding destabilizes, at least partially, the reduced state.[10,11]

Solomon and co-workers have provided a detailed picture of the electronic structure of the metal ion in blue copper sites.[4] These studies led them to classify type 1 sites as "classic" and "perturbed" sites.[4,12] Classic blue copper sites (those present in plastocyanin, amicyanin, and azurin) exhibit an intense absorption feature at ∼600 nm, a weak band at ∼450 nm, and axial EPR spectra. These centers are characterized by a weak bonding interaction with an axial methionine ligand.[1−6] Perturbed centers can be distinguished by an increased absorption of the 450 nm band (with a concomitant decrease in the 600 nm blue band intensity) and rhombic EPR spectra. These perturbations are generally attributed to stronger copper−axial ligand interactions.[13] Perturbed centers can arise from a tetrahedral distortion, when a Gln ligand replaces the Met (stellacyanin), or from a tetragonal distortion with an axial Met ligand (pseudoazurin, cucumber basic protein, and nitrite reductase). Nitrite reductases (NiRs) have recently offered an opportunity to study an "ultimate" tetragonally perturbed site (green), where two classes of nitrite reductases (green and blue) have been crystallographically characterized.[14,15] The structures of the type 1 Cu sites of the green and blue NiRs resemble each other very closely. There are only small differences in the Cu−ligand distances, including those for methionine, in which such differences had been suggested as a reason for the differences in color.[16] Previously, the dominant geometric factor affecting the electronic structure

was proposed to be coupled angular changes in the positions of the Cys and Met ligands.[17] In blue NiRs, there is a lateral displacement (0.76 Å) of the methionine ligand with respect to its position in the green NiRs, which produces angular differences between the two sites.[15] However, the two structures show no difference in their Cys−Cu−Met angles, but the HisC−Cu−Met angle is 115° in the blue vs 132° in the green nitrite reductase. [Note: HisC and HisN refer to the C- and N-terminal histidine ligands, respectively.] For both of these, displacement of the Cu atom with respect to the strong ligands is essentially the same (0.5 Å in blue NiR vs 0.6 Å in green NiR). Dodd et al.[15] have proposed that the HisC−Cu−Met angle, among other subtle factors, accounts for the differences in color for the two groups of NiRs which contain an otherwise "classical" blue Cu center. Solomon et al. have proposed that deviation from a $C_{3v}$ geometry toward tetragonal distortion in type 1 copper(II) centers can be quantified by the angle $\phi$ between the $N_{His}CuN_{His}$ and $S_{Cys}CuS_{Met}$ planes.[4,12]

NMR is able to probe the electronic structure of each copper−ligand interaction, allowing us to extend further our understanding of the spectroscopic and thermodynamic properties of copper(II) in BCPs, and facilitate the rationalization of how the protein folding and the environment determine the metal site geometry. The oxidized state of BCPs is paramagnetic.[18] NMR has proven to be a fruitful technique for the study of the paramagnetic centers of electron-transfer metalloproteins such as cytochromes and iron−sulfur proteins, since it yields information on the electron spin density on the metal ligands, providing a complementary view of the electronic structure of these metal sites.[19,20] In the past few years, the study of copper(II) centers has been advanced by work from the laboratories of Canters and Bertini,[21−24] opening the possibility of retrieving the unpaired spin density in all copper ligands without the need for metal substitution.[25−34]

(8) Malmström, B. G. *Eur. J. Biochem.* **1994**, *233*, 711−718.
(9) Guckert, G. A.; Lowery, M. D.; Solomon, E. I. *J. Am. Chem. Soc.* **1995**, *117*, 2817−2844.
(10) Winkler, J.; Wittung-Stafshede, P.; Leckner, J.; Malmström, B.; Gray, H. *Proc. Natl. Acad. Sci. U.S.A.* **1997**, *94*, 4246−4249.
(11) Wittung-Stafshede, P.; Hill, M. G.; Gomez, E.; Di Bilio, A. J.; Karlson, B. G.; Leckner, J.; Winkler, J. R.; Gray, H. B.; Malmström, B. *J. Biol. Inorg. Chem.* **1998**, *3*, 367−370.
(12) LaCroix, L. B.; Randall, D. W.; Nersissian, A. M.; Hoitink, C. W. G.; Canters, G. W.; Valentine, J. S.; Solomon, E. I. *J. Am. Chem. Soc.* **1998**, *120*, 9621−9631.
(13) van Gastel, M.; Canters, G. W.; Krupka, H.; Messerschimdt, A.; de Waal, E. C.; Warmerdam, G. C. M.; Groenen, E. J. J. *J. Am. Chem. Soc.* **2000**, *122*, 2322−2328.
(14) Murphy, M. E.; Turley, S.; Kukimoto, M.; Nishiyama, M.; Horinouchi, S.; Sasaki, H.; Tanokura, M.; Adman, E. T. *Biochemistry* **1995**, *34*, 12107−12117.
(15) Dodd, F. E.; Van Beeumen, J.; Eady, R. R.; Hasnain, S. S. *J. Mol. Biol.* **1998**, *282*, 369−382.

(16) Adman, E. T.; Godden, J. E.; Turley, S. *J. Biol. Chem.* **1995**, *270*, 27458−27474.
(17) LaCroix, L. B.; Shadle, S. E.; Wang, Y. N.; Averill, B. A.; Hedman, B.; Hodgson, K. O.; Solomon, E. I. *J. Am. Chem. Soc.* **1996**, *118*, 7755−7768.
(18) Banci, L.; Pierattelli, R.; Vila, A. J. *Adv. Protein Chem.* **2002**, in press.
(19) Bertini, I.; Turano, P.; Vila, A. J. *Chem. Rev.* **1993**, *93*, 2833−2932.
(20) Bertini, I.; Luchinat, C. *NMR of paramagnetic substances*, 1st ed.; Coordination Chemistry Reviews 150; Elsevier: Amsterdam, 1996.
(21) Kalverda, A. P.; Salgado, J.; Dennison, C.; Canters, G. W. *Biochemistry* **1996**, *35*, 3085−3092.
(22) Bertini, I.; Ciurli, S.; Dikiy, A.; Luchinat, C.; Martini, G.; Safarov, N. *J. Am. Chem. Soc.* **1999**, *121*, 2037−2046.
(23) Bertini, I.; Fernandez, C. O.; Karlson, B. G.; Leckner, J.; Luchinat, C.; Malmström, B. G.; Nersissian, A. M.; Pierattelli, R.; Shipp, E.; Valentine, J., S.; Vila, A. J. *J. Am. Chem. Soc.* **2000**, *122*, 3701−3707.
(24) Bertini, I.; Bryant, D. A.; Ciurli, S.; Dikiy, A.; Fernandez, C. O.; Luchinat, C.; Safarov, N.; Vila, A. J.; Zhao, J. *J. Biol. Chem.* **2001**, *276*, 47217−47226.
(25) Moratal Mascarell, J. M.; Salgado, J.; Donaire, A.; Jimenez, H. R.; Castells, J. *Inorg. Chem.* **1993**, *32*, 3587−3588.
(26) Vila, A. J. *FEBS Lett.* **1994**, *355*, 15−18.
(27) Salgado, J.; Jimenez, H. R.; Donaire, A.; Moratal, J. M. *Eur. J. Biochem.* **1995**, *231*, 358−369.
(28) Piccioli, M.; Luchinat, C.; Mizoguchi, T. J.; Ramirez, B. E.; Gray, H. B.; Richards, J. H. *Inorg. Chem.* **1995**, *34*, 737−742.
(29) Vila, A. J.; Fernandez, C. O. *J. Am. Chem. Soc.* **1996**, *118*, 7291−7298.
(30) Salgado, J.; Jimenez, H. R.; Moratal, J. M.; Kroes, S. J.; Warmerdam, G. C. M.; Canters, G. W. *Biochemistry* **1996**, *35*, 1810−1819.
(31) Fernandez, C. O.; Sannazzaro, A. I.; Vila, A. J. *Biochemistry* **1997**, *36*, 10566−10570.
(32) Donaire, A.; Salgado, J.; Moratal, J. M. *Biochemistry* **1998**, *37*, 8659−8673.
(33) Salgado, J.; Kroes, S. J.; Berg, A.; Moratal, J. M.; Canters, G. W. *J. Biol. Chem.* **1998**, *273*, 177−185.
(34) Salgado, J.; Kalverda, A. P.; Diederix, R. E. M.; Canters, G. W.; Moratal, J. M.; Lawler, A. T.; Dennison, C. *J. Biol. Inorg. Chem.* **1999**, *4*, 457−467.

Cu(II)−plastocyanin (Pc),[22] Cu(II)−azurin (Az), and Cu(II)−stellacyanin (St)[23] have been studied with these techniques. These studies have provided direct evidence of the interplay between the strength of the copper−axial ligand interaction and the copper−Cys covalence (which is reflected in large variations in the observed shifts of the Cys proton resonances). This behavior was described for the classic blue sites (plastocyanin and azurin) or tetrahedrally perturbed sites (stellacyanin). In tetragonally perturbed blue copper centers, the axial Met ligand is generally closer to the copper ion than in classic sites, with the main perturbation arising from a different orientation of the Cys and Met ligands with respect to the His residues.[4]

No NMR study of blue sites with tetragonal distortion has been reported. Therefore, we decided to study two BCPs with tetragonally distorted copper sites, pseudoazurin (PsAz)[35] and rusticyanin (Rc),[36−39] by performing ^{1}H NMR spectroscopy of the oxidized species at high magnetic fields (18.8 T). The absorption and EPR spectra of PsAz and Rc are similar, even though there are significant differences in the Cu−$S_\gamma$(Cys) and Cu−$S_\delta$(Met) bond lengths.[40,41] NMR experiments were thus designed to explore the similarities and subtle differences between these two closely related copper sites, which could then be analyzed in the context of the BCPs family. An additional reason for the interest in studying Rc was its high redox potential (680 mV),[39,42] which has been attributed to the highly hydrophobic environment of the metal site[36,41,43,44] and the presence of a serine next to the N-terminal His ligand.[45,46]

In this work, we address the following issues: (1) Can the subtle differences between PsAz and Rc be monitored by NMR, and what can be learned from this spectroscopy? (2) How does the tetragonal distortion in blue copper sites impact the unpaired spin density in the metal ligands? (3) Is there a correlation between the chemical shifts of the Cys protons and the geometrical features of the Cu(II)−Cys moiety in different BCPs? (4) Are there structural factors in the metal site geometry that contribute to a high redox potential in Rc?

## Materials and Methods

**Protein Purification and Metal Derivatives.** Pseudoazurin from *Achromobacter cycloclastes* IAM 1013 was purified as previously described.[47] The final absorbance ratio $A_{282}/A_{594}$ was 1.45. Recombinant rusticyanin from *Thiobacillus ferrooxidans* was expressed and purified from transformed *Escherichia coli* strains BL21(DE3) cultures as already described.[39]

(35) Ambler, R. P.; Tobari, J. *Biochem. J.* **1985**, *232*, 451−457.
(36) Hall, J. F.; Kanbi, L. D.; Strange, R. W.; Hasnain, S. S. *Biochemistry* **1999**, *38*, 12675−12680.
(37) Ingledew, W. J.; Cox, J. C.; Halling, P. J. *FEMS Microbiol. Lett.* **1977**, *2*, 193−197.
(38) Djebli, A.; Proctor, P.; Blake, R. C., II; Shoham, M. *J. Mol. Biol.* **1992**, *227*, 581−582.
(39) Hall, J. F.; Hasnain, S. S.; Ingledew, W. J. *FEMS Microbiol. Lett.* **1996**, *137*, 85−89.
(40) Inoue, T.; Nishio, N.; Suzuki, S.; Kataoka, K.; Kohzuma, T.; Kai, Y. *J. Biol. Chem.* **1999**, *274*, 17845−17852.
(41) Walter, R. L.; Ealick, S. E.; Friedman, A. M.; Blake, R. C., II.; Proctor, P.; Shoham, M. *J. Mol. Biol.* **1996**, *263*, 730−751.
(42) Cox, J. C.; Boxer, D. H. *Biochem. J.* **1978**, *174*, 497−502.
(43) Botuyan, M. A.; Toy-Palmer, A.; Chung, J.; Blake, R. C.; Beroza, P.; Case, D. A.; Dyson, H. J. *J. Mol. Biol.* **1996**, *263*, 752−767.
(44) Donaire, A.; Jiménez, B.; Moratal, J. M.; Hall, J. F.; Hasnain, S. S. *Biochemistry* **2001**, *40*, 837−846.
(45) Grossmann, J. G.; Ingledew, W. J.; Harvey, I.; Strange, R. W.; Hasnain, S. S. *Biochemistry* **1995**, *34*, 8406−8414.
(46) Hall, J. F.; Kanbi, L. D.; Harvey, I.; Murphy, L. M. M.; Hasnain, S. S. *Biochemistry* **1998**, *37*, 11451−11458.
(47) Kohzuma, T.; Yamada, H.; Deligeer, M.; Suzuki, S. *J. Elect. Anal. Chem.* **1997**, *438*, 49−53.

**NMR Spectroscopy.** Samples (∼2−5 mM) for NMR experiments were concentrated using Centricon-10 (Millipore) units. A small amount of reduced protein (≤5%) was enough to perform the exchange NMR experiments. $D_2O$ solutions were prepared by exchanging the solvent in Centricon-10 units. All chemical shifts were referenced to the chemical shift of the residual water (HOD) at the appropriate temperature according to the relationship $\delta_{HOD} = -0.012t + 5.11$ ppm, where $t$ is the temperature (in °C).[48]

NMR spectra were recorded on an Avance 800 spectrometer operating at a proton frequency of 800.13 MHz. Saturation-transfer experiments in solutions containing Cu(II)− and Cu(I)−pseudoazurin or rusticyanin were performed using an *on*−*off* scheme where *on* values varied from −100 to 2000 ppm and *off* values were positioned symmetrically to the *on* values with respect either to the residual water signal or to the medium values of the $\beta$-$CH_2$ Cys chemical shifts in the reduced form, to avoid off-resonance effects.[22] A prototype 2.5 mm large bandwidth detection probe with a 2 $\mu$s, 90° pulse was employed in these experiments. The power used for saturation-transfer experiments on the $\beta$-$CH_2$ Cys protons was 1.8 W, applied for 5−20 ms. Irradiation of the hyperfine-shifted signals corresponding to the Cu(II) species was achieved by using power levels ranging from 0.002 to 0.2 W.

**Analysis of the Hyperfine Shifts.** Interpretation of the NMR spectra of paramagnetic species depends on the evaluation of the different contributions to the observed chemical shifts, $\delta_{obs}$:[20,49−51]

$$\delta_{obs} = \delta_{dia} + \delta_{con} + \delta_{pc} \qquad (1)$$

where $\delta_{dia}$ is the chemical shift of the observed nucleus in an analogous diamagnetic system, $\delta_{con}$ is the Fermi contact shift due to the unpaired electron density on the nucleus of interest, and $\delta_{pc}$ represents the pseudocontact shift induced by the magnetic anisotropy of the unpaired electron(s) residing on the metal ion. In the present case, $\delta_{dia}$ values are directly measured in the saturation-transfer experiment under the same experimental conditions in which $\delta_{obs}$ is retrieved. In the case of rusticyanin, these values are in agreement with those previously reported.[52]

The pseudocontact contribution ($\delta_{pc}$) can be evaluated using information derived from the protein structure and the magnetic susceptibility anisotropy tensor, or from the *g* tensor (whose square is proportional to the $\chi$ tensor for $S = {}^1/_2$ systems with an isolated orbitally nondegenerate ground state). By assuming axial *g* tensors (which is a reasonably good approximation for these systems),[14,17,18,29] $\delta_{pc}$ is given by[49,50]

$$\delta_{pc} = \frac{\mu_0}{4\pi}\frac{\mu_B^2 S(S+1)}{9kTr^3}(3\cos^2\theta - 1)(g_{\parallel}^2 - g_{\perp}^2) \times 10^6 \qquad (2)$$

where $\mu_0$ is the magnetic permeability in a vacuum, $\mu_B$ is the electron Bohr magneton, $k$ is Boltzmann's constant, $T$ is the absolute temperature, $r$ is the proton−copper distance, $\theta$ is the angle between the metal−proton vector and the magnetic *z* axis, and the *g* tensor parameters are defined by $g_{\parallel} = g_{zz}$ and $g_{\perp} = (g_{xx} + g_{yy})/2$. Even though there is a non-negligible unpaired electron density on the sulfur atom, we have calculated the pseudocontact shift on the basis of the metal-centered approximation, which has been demonstrated to be valid for these systems.[22] The values used for the *g* components were $g_{xx} = 2.02$, $g_{yy} = 2.09$, and $g_{zz} = 2.20$ for pseudoazurin,[53] and $g_{xx} = 2.02$, $g_{yy} = 2.06$, and $g_{zz} = 2.21$, for rusticyanin.[39] The *g* tensor orientation has

(48) Bertini, I.; Ciurli, S.; Dikiy, A.; Luchinat, C. *J. Am. Chem. Soc.* **1993**, *115*, 12020−12028.
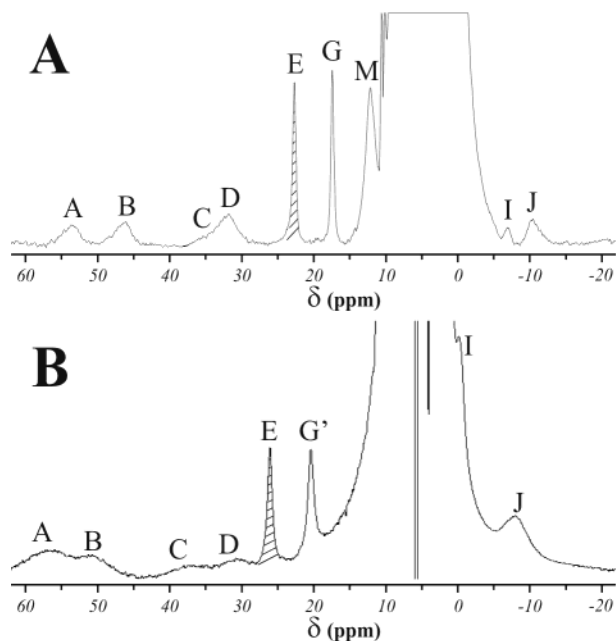(49) McConnell, H. M.; Robertson, R. E. *J. Chem. Phys.* **1958**, *29*, 1361−1365.
(50) McConnell, H. M.; Chesnut, D. B. *J. Chem. Phys.* **1958**, *28*, 107−117.
(51) Kurland, R. J.; McGarvey, B. R. *J. Magn. Reson.* **1970**, *2*, 286−301.
(52) Hunt, A. H.; Toy-Palmer, A.; Cavanagh, J.; Blake, R. C., II; Dyson, H. J. *J. Mol. Biol.* **1994**, *244*, 370−384.
(53) Suzuki, J.; Sakurai, T.; Shidara, S.; Iwasaki, H. *Inorg. Chem.* **1989**, *28*, 802−804.

**Figure 2.** ^{1}H NMR (800 MHz) spectra of (A) Cu(II)−pseudoazurin (100 mM Tris-HCl at pH 8.0 in H$_2$O at 298 K) and (B) Cu(II)−rusticyanin (100 mM acetate buffer at pH 5.5 in H$_2$O at 296 K). Shadowed signals totally (PsAz) or partially (Rc) disappear when the spectrum is recorded in D$_2$O (see text).

been assumed to be similar to those found for plastocyanin[54] and azurin[55] by overlaying the copper ion and the bound N(His) atoms. Variations derived from different orientations of this tensor are expected to be within ±50% of the calculated $\delta_{pc}$ values.[21−23] Since $\delta_{pc}$ is smaller than 3.2 ppm for all protons,[21−23] differences due to tensor orientation remain negligible in all cases.

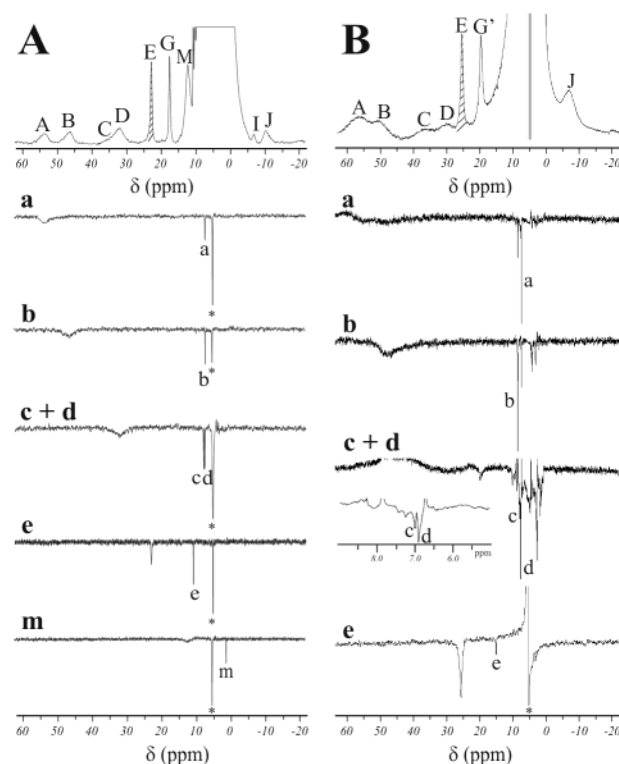The hyperfine coupling constants for each nucleus ($A/h$) can be calculated from the following equation:[49,50]

$$\frac{A}{h} = \frac{1}{2\pi} \frac{\delta_{con} 3\gamma_N kT}{g_{av}\mu_B S(S+1)} \tag{3}$$

where $\gamma_N$ is the nuclear magnetogyric ratio and $g_{av}$ is the average $g$ value.

### Results

**Cu(II)−Pseudoazurin.** The ^{1}H NMR spectrum of Cu(II)−pseudoazurin in H$_2$O at 800 MHz is shown in Figure 2A. Seven downfield-shifted (A−G, M) and two upfield-shifted signals (I, J) were detected outside the diamagnetic envelope (we have maintained the signal labeling used previously in related systems).[22,23] The spectrum is similar to that already reported,[56] with improved resolution due to the high field, that allows us to fully assign the hyperfine shifted resonances.

Signal E is absent when the spectrum is recorded in D$_2$O solution. Resonances A−M were assigned through saturation-transfer experiments performed on a sample of oxidized pseudoazurin containing ca. 5% of the reduced species. Irradiation of resonances A−D gave saturation transfer with signals at 7.0, 6.8, 7.5, and 7.2 ppm, respectively (Figure 3A). From the observed diamagnetic shifts of these resonances, we conclude

(54) Penfield, K. W.; Gewirth, A. A.; Solomon, E. I. *J. Am. Chem. Soc.* **1985**, *107*, 4519−4529.
(55) Coremans, J. W. A.; Poluektov, O. G.; Groenen, E. J. J.; Canters, G. W.; Nar, H.; Messerschmidt, A. *J. Am. Chem. Soc.* **1994**, *116*, 3097−3101.
(56) Sato, K.; Dennison, C. *Biochemistry* **2002**, *41*, 120−130.

**Figure 3.** ^{1}H NMR (800 MHz) saturation-transfer spectra of (A) Cu(II)−pseudoazurin and (B) Cu(II)−rusticyanin. The irradiated signals are indicated in each trace with lowercase letters. The upper trace represents the reference spectrum. The signal marked with an asterisk corresponds to the H$_2$O resonance. Conditions are the same as in Figure 2. The inset in Figure 3B (c + d) shows the expanded 5−9 ppm region.

**Table 1.** Hyperfine-Shifted Signals Corresponding to Copper Ligands in Cu(II)− and Cu(I)−Pseudoazurin Recorded at 800 MHz in 100 mM Tris-HCl at pH 8.0 and 298 K

| signal | assignments | $\delta$(ppm)$_{ox}$ | $\delta$(ppm)$_{red}$ |
|---|---|---|---|
| | H$\beta$ Cys78 | 510 ± 70 | 2.8 |
| | H$\beta'$ Cys78 | 390 ± 50 | 3.1 |
| A | H$\delta$2 His81 | 53.5 | 7.0 |
| B | H$\delta$2 His40 | 46.1 | 6.8 |
| C | H$\epsilon$1 His40 | 32.0 | 7.5 |
| D | H$\epsilon$1 His81 | 32.0 | 7.2 |
| E | H$\epsilon$2 His40 | 23.0 | 10.5 |
| G | H$\alpha$ Asn41 | 17.4 | 4.9 |
| M | $\epsilon$-CH$_3$ Met86 | 12.1 | 0.8 |
| | NH Asn41 | −15.0 ± 4.0 | 9.6 |

that signals A−D correspond to the nonexchangeable H$\delta$2 and H$\epsilon$1 protons of His40 and His81 (Table 1). Irradiation of the only exchangeable hyperfine-shifted signal (E) yielded a saturation transfer with a resonance at 10.5 ppm, which we assign to the exchangeable H$\epsilon$2 proton of the most buried histidine ligand, His40. No resonance corresponding to the H$\epsilon$2 imidazole proton of the exposed His81 is observed, in agreement with the spectroscopic data on amicyanin, azurin, and plastocyanin.[21−24] The assignments of the imidazole His resonances concur with those previously reported in these proteins.

Signal G displayed a saturation transfer with a resonance located at 4.9 ppm (not shown). The chemical shifts of this nucleus in both oxidation states are coincident with similar signals attributed to the H$\alpha$ of an Asn residue next to one of the His ligands (Asn41 in this protein).[22,23] Signal M showed a saturation transfer with a signal located at 0.8 ppm (Figure 3). Both the intensity of this signal and the chemical shift of the
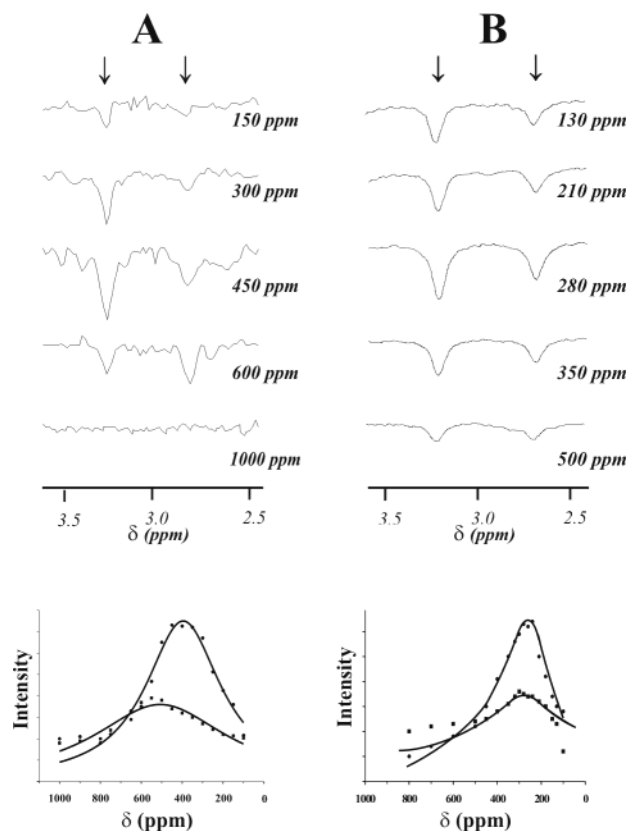
**Figure 4.** Reconstructed ${}^1$H NMR (800 MHz) spectrum containing signals not observable in the normal spectrum. The positions and line widths of these signals were obtained by plotting the intensity of the respective exchange connections with the reduced species (●, ■) as a function of the decoupler irradiation frequency, and by fitting these values to a Lorentzian function (indicated as a continuous line in the plot): $\beta$-CH$_2$ Cys signals in (A) Cu(II)−pseudoazurin and (B) Cu(II)−rusticyanin.

reduced counterpart suggest that it corresponds to a methyl group. The only candidate for this signal, therefore, is the $\epsilon$-CH$_3$ from Met86. The positions of all diamagnetic signals in the reduced protein detected through saturation-transfer experiments are similar to those found in *Paracoccus pantotrophus* Cu(I)−pseudoazurin,[57] confirming the present assignments.

To locate the fast-relaxing resonances, a blind saturation-transfer experiment was performed.[22] A very large spectral window was sampled in steps of 50−100 ppm. Observation of the build-up and decay of the signal intensity as a function of the sampled frequency provided the precise location of these extremely broad signals (Figure 4A). Two downfield resonances were located at 510 ± 70 and 390 ± 50 ppm, according to the profiles shown in Figure 4A, that we assign as the $\beta$-CH$_2$ protons of Cys78 on the basis of their large chemical shifts and line widths.[22,23] When the upfield region was irradiated, a saturation transfer was observed with a signal at 9.6 ppm, the maximum intensity of which corresponded to irradiation at −15 ppm (not shown). By analogy with ${}^1$H NMR studies on related proteins, we attribute this resonance to the peptide NH of Asn41.[22,23]

**Cu(II)−Rusticyanin.** The ${}^1$H NMR spectrum of rusticyanin recorded in H$_2$O at 800 MHz is shown in Figure 2B. Six downfield signals (A−E, G′) can be located outside the diamagnetic envelope, whereas two resonances (I, J) are found

(57) Thompson, G. S.; Leung, Y. C.; Ferguson, S. J.; Radford, S. E.; Redfield, C. *Protein Sci.* **2000**, *9*, 846−858.

**Table 2.** Hyperfine-Shifted Signals Corresponding to Copper Ligands in Cu(II)− and Cu(I)−Rusticyanin Recorded at 800 MHz in 100 mM Acetate Buffer at pH 5.5 and 296 K

| signal | assignments | $\delta$(ppm)$_{ox}$ | $\delta$(ppm)$_{red}$ |
|---|---|---|---|
| | H$\beta$ Cys | 240 ± 20 | 3.2 |
| | H$\beta'$ Cys | 300 ± 50 | 2.7 |
| A | H$\delta$2 His143 | 58.1 | 6.7 |
| B | H$\delta$2 His85 | 50.2 | 7.9 |
| C | H$\epsilon$1 His85 | 36.7 | 7.1 |
| D | H$\epsilon$1 His143 | 30.3 | 7.0 |
| E | H$\epsilon$2 His85 | 25.3 | 14.5 |
| G′ | H$\alpha$ Ser86 | 19.5 | 5.0 |
| M | $\epsilon$-CH$_3$ Met148 | 8.1 | 0.8 |
| | NH Ser86 | −20.0 ± 4.0 | 10.6 |

in the upfield portion of the spectrum. Signal E exhibits a fractional intensity when the spectrum is recorded in D$_2$O. A detailed analysis of the superWEFT spectrum in the diamagnetic envelope reveals a fast-relaxing broad signal (M) at 8.1 ppm (not shown). The intensity of this signal is not altered when the spectrum is recorded in D$_2$O.

The paramagnetically shifted signals were assigned on the basis of 1D exchange spectroscopy on a partially (3%) reduced sample (Figure 3B). Irradiation of signals A and B gave saturation transfer with signals at 6.7 and 7.9 ppm, corresponding to the chemical shifts of the H$\delta$2 protons of His143 and His85 in the reduced species,[52] respectively (Table 2). Irradiation of signals C and D gave saturation transfer with signals at 7.1 and 7.0 ppm, assigned to the H$\epsilon$1 protons of the histidine ligands. An irradiation profile performed in steps of 3 ppm in this region (40−20 ppm) allowed us to unequivocally assign signals C and D as the H$\epsilon$1 protons of His85 and His143, respectively (data not shown). When signal E was irradiated, a saturation transfer was observed at 14.5 ppm (Figure 3B), indicating that this signal corresponds to the H$\epsilon$2 proton of His85. Signals G′, I, and J gave saturation transfer with signals at 5.0, 2.6, and 5.1 ppm that correspond to the chemical shifts of the H$\alpha$ of Ser86, H$\beta$1 of His143, and H$\alpha$ of Cys138, respectively.[52] These assignments are coincident with those from Cu(II)−PsAz (see above) and are analogous to those previously reported for other Cu(II) BCPs.[21−23] As mentioned above, a fast-relaxing signal at 8.1 ppm can be detected. This signal is absent in the superWEFT spectrum of several Cu(II)Rc mutants in which the axial methionine has been replaced by another amino acid (A. Donaire, unpublished). Hence, we tentatively assign this signal as the $\epsilon$-CH$_3$ from Met148.

Blind saturation-transfer experiments were performed to locate the $\beta$-CH$_2$ Cys signals. The profile of the irradiation response for these resonances is shown in Figure 4B. Fitting of these profiles to Lorentzian functions yields maxima at 300 ± 50 and 240 ± 20 ppm. Blind NOE experiments, irradiating close to −20 ppm, gave a response at 10.6 ppm (not shown). This chemical shift corresponds to the amide NH of Ser86 in the reduced form.[52] This saturation transfer was observed in experiments performed in D$_2$O, indicating that this proton is not easily exchangeable with bulk solvent. This finding supports this assignment, since the Ser86 NH amide proton is hydrogen-bonded to the S$_\gamma$(Cys) atom in rusticyanin.[41,43]

## Discussion

**Analysis of the NMR Spectra.** The ${}^1$H NMR spectra of Cu(II)−PsAz and Cu(II)−Rc resemble those reported for other

***Table 3.*** Diamagnetic, Pseudocontact, and Contact Contribution to the Chemical Shifts (in ppm) of Protons Belonging to Coordinated Residues for Oxidized PsAz and Rc, as Well as Contact Contributions of the Analogous Protons for Oxidized Pc, Az, St, and Am and the Average Values for $\beta$-CH$_2$ Cys Observed Shifts, $\delta_{1/2}$

| proton | PsAz, 298 K, pH 8 (this work) | | | | Rc, 296 K, pH 5.5 (this work) | | | | Pc,[a] 298 K, pH 7.5 | Az,[b] 278 K, pH 8.0 | St,[b] 301 K, pH 6.0 | Am,[c] 308 K, pH 7.0 |
|---|---|---|---|---|---|---|---|---|---|---|---|---|
| | $\delta_{obs}$ | $\delta_{dia}$ | $\delta_{pc}$ | $\delta_{con}$ | $\delta_{obs}$ | $\delta_{dia}$ | $\delta_{pc}$ | $\delta_{con}$ | $\delta_{con}$ | $\delta_{con}$ | $\delta_{con}$ | $\delta_{con}$ |
| Cys H$\beta$1 | 510 | 2.8 | −0.9 | 508 | 300 | 2.7 | 0.8 | 297 | 650 | 850 | 450 | |
| H$\beta$2 | 390 | 3.1 | 0.5 | 386 | 240 | 3.2 | 0.8 | 236 | 490 | 800 | 370 | |
| $\delta_{1/2}$ | 450 | | | | 270 | | | | 570 | 825 | 410 | |
| H$\alpha$ | e | | | | −8.9 | 5.1 | −0.7 | −13.3 | −12.3 | −11.5 | −11.4 | −12.9[g] |
| HisN H$\delta$2 | 46.1 | 6.8 | −0.7 | 40.0 | 50.2 | 7.9 | −0.8 | 43.1 | 40.5 | 44.5 | 42.2[d] | 36.6 |
| H$\epsilon$1 | 32.0 | 7.5 | −3.1 | 27.6 | 36.7 | 7.1 | −3.5 | 33.1 | 31.9 | 44.4[d] | 39.0[d] | |
| HN$\epsilon$2 | 23.0 | 10.5 | −0.8 | 13.3 | 25.3 | 14.5 | −0.9 | 11.7 | 20.7 | 16.7 | 17.0 | 14.9 |
| HisC H$\delta$2 | 53.5 | 7.0 | −0.8 | 47.3 | 58.1 | 6.7 | −0.9 | 52.3 | 45.5 | 48.2 | 49.0[d] | 43.5 |
| H$\epsilon$1 | 32.0 | 7.2 | 1.3 | 23.5 | 30.3 | 7.0 | 1.6 | 21.7 | 28.2 | 30.6[d] | 27.8[d] | |
| Met $\epsilon$-CH$_3$ | 12.1 | 0.8 | 0.8 | 10.5 | 8.1 | 0.8 | 1.3 | 6.0 | e | e | e | e |
| H$\gamma$1 | e | | | | e | | | | | 8.6 | | 6.7[f] |
| H$\gamma$2 | e | | | | e | | | | | 19.9 | | 7.3[f] |
| Asn/Ser | | | | | | | | | | | | |
| HN | −15.0 | 9.6 | −1.2 | −23.4 | −20.0 | 10.6 | −1.7 | −28.9 | −28.4 | −39.0 | −22.0 | |
| H$\alpha$ | 17.4 | 4.9 | −0.4 | 12.7 | 19.5 | 5.0 | −0.4 | 14.9 | 13.1 | 15.5 | 13.0 | 9.4[g] |

[a] Pc (plastocyanin), from ref 22. [b] Az (azurin) and St (stellacyanin), from ref 23. [c] Am (Amicyanin), from ref 21. [d] Sequence-specific assignment for these protons is tentatively proposed in this work (see text). [e] Not observed. [f] Assignments may be exchanged. [g] Calculated in this work, from the $\delta_{obs}$ values reported in ref 21.

***Table 4.*** Hyperfine Coupling Constants in BCPs

| | $A/h$ (MHz) | | | | | |
|---|---|---|---|---|---|---|
| proton | PsAz (this work) | Rc (this work) | Pc[a] | Az[b] | St[b] | Am[c] |
| Cys H$\beta$ | 18 | 11 | 23 | 28/27 | 16/13 | |
| H$\beta'$ | 14 | 8 | 17 | 27/28 | 13/16 | |
| H$\alpha$ | | | −0.47 | −0.44 | −0.38 | −0.41 | −0.46[d] |
| HisN H$\delta$2 | 1.43 | 1.55 | 1.45 | 1.49 | 1.53 | 1.31 |
| H$\epsilon$1 | 0.99 | 1.19 | 1.14 | 1.48 | 1.40 | |
| H$\epsilon$2 | 0.48 | 0.42 | 0.74 | 0.56 | 0.62 | |
| HisC H$\delta$2 | 1.69 | 1.87 | 1.63 | 1.61 | 1.77 | 1.56 |
| H$\epsilon$1 | 0.85 | 0.77 | 1.01 | 1.02 | 1.01 | |
| Met $\epsilon$-CH$_3$ | 0.37 | 0.22 | | | | |
| Asn/Ser HN | −0.78 | −1.06 | −1.02 | −1.3 | −0.8 | |
| H$\alpha$ | 0.45 | 0.54 | 0.47 | 0.52 | 0.47 | 0.34[d] |

[a] From ref 22. [b] From ref 23. [c] From ref 21. [d] Calculated in this work, from the $\delta_{obs}$ values reported in ref 21.

oxidized BCPs (amicyanin, plastocyanin, azurin, and stellacyanin).[21−23] The histidine signals display similar spectral features in all studied cupredoxins, whereas those resonances corresponding to the cysteine and axial ligand(s) vary among different proteins, reflecting changes in the electronic structure of the metal site. It has been shown that, in classic and tetrahedrally distorted blue sites, the Cu(II)−Cys interaction depends on the axial ligand(s):[23] a stronger axial ligand (such as in stellacyanin) reduces the Cu(II)−S$_\gamma$(Cys) covalence,[12] thus giving rise to a much smaller electron spin density on the $\beta$-CH$_2$ Cys protons. Along this line, we would like to analyze how the tetragonal distortion in PsAz and Rc affects the unpaired spin density in the different copper ligands.

The electron spin density on the copper ligand nuclei was calculated as described in the Materials and Methods section. Table 3 displays the calculated pseudocontact ($\delta_{pc}$) and contact ($\delta_{con}$) shifts for pseudoazurin and rusticyanin, compared to those from other BCPs. Table 4 summarizes the hyperfine coupling constants ($A/h$) for the protons of the coordinated residues obtained by applying eq 3. In the following sections, we will discuss these parameters in comparison to those from other oxidized BCPs studied by NMR spectroscopy (amicyanin,[21] plastocyanin,[22] azurin, and stellacyanin[23]).

**(a) His Signals.** Comparison of the NMR features of the imidazole His signals in different BCPs reveal that their $\delta_{con}$ values are H$\delta$2 (HisC) > H$\delta$2 (HisN) > H$\epsilon$1 (HisN) > H$\epsilon$1 (HisC) > H$\epsilon$2 (HisN) (Table 3). For the three observable histidine protons in all BCPs, the contact shifts follow the trend H$\delta$2 > H$\epsilon$1 > H$\epsilon$2, which holds for both His ligands. On the basis of these observations, we suggest a sequence-specific assignment for the His resonances in azurin and stellacyanin,[23] as indicated in Table 3. In the case of azurin, these assignments are supported by ENDOR/ESEEM data.[58]
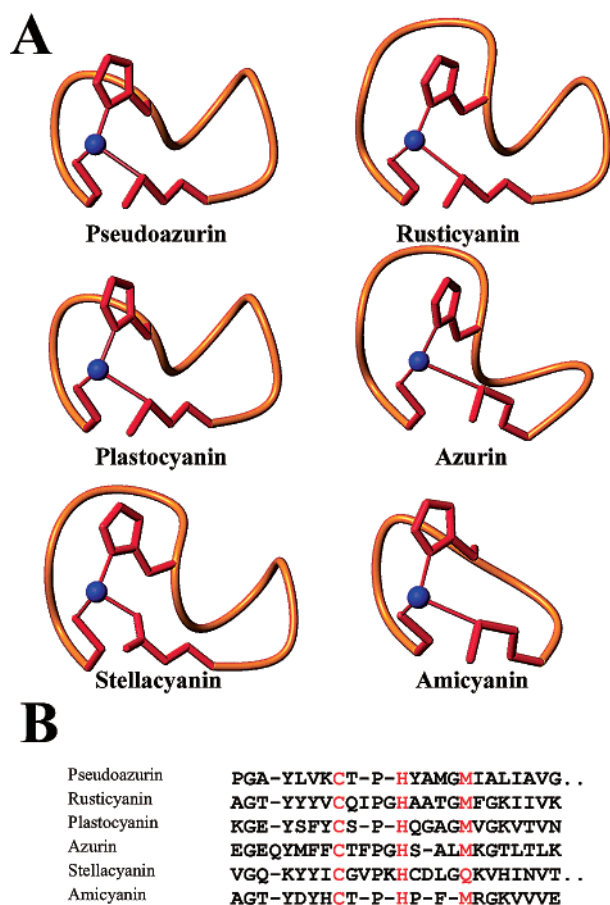
The $\delta_{con}$ values for each type of proton (except the H$\epsilon$1 signals of azurin) span rather narrow shift ranges, for both HisN and HisC resonances. These observations indicate that (1) the unpaired spin density in both histidine ligands is fairly constant in the different blue copper proteins, in both classic and distorted sites, and (2) the same electron delocalization pattern is operative in both histidine ligands. These conclusions are feasible, provided the orientation of the copper orbitals in the *xy* plane with respect to the histidine ligands is similar in all blue sites. Van Gastel et al. recently pointed out that the magnetic *z* axis in different BCPs is nearly perpendicular to the plane defined by the copper ion and the coordinated N$\delta$1(His).[13] Our results provide further support for this proposal.

The environments of HisN and HisC are different in different BCPs. HisC is solvent-exposed, being located in the middle of a loop connecting two $\beta$-strands,[59] distinguished by different lengths and conformations in each blue copper protein (Figure 5). HisN is invariably buried in the protein structure. The relatively small variation in chemical shifts observed for the imidazole protons of both of the His ligands among the BCPs suggests that their orientation is conserved in BCPs. This is not unexpected for HisN, but it indicates that HisC is sufficiently flexible to accommodate its conformation in such a way as to give rise to a similar copper−N$\delta$1 interaction in all BCPs (Figure 5).[60−63]

(58) van Gastel, M.; Coremans, J. W. A.; Jeuken, L.; Canters, G. W.; Groenen, E. J. J. *J. Phys. Chem. A* **1998**, *102*, 4462−4470.
(59) Buning, C.; Canters, G. W.; Comba, P.; Dennison, C.; Jeuken, L.; Melter, M.; Sanders-Loehr, J. *J. Am. Chem. Soc.* **2000**, *122*, 204−211.
(60) Baker, E. N. *J. Mol. Biol.* **1988**, *203*, 1071.

## A



Pseudoazurin

Rusticyanin

Plastocyanin

Azurin

Stellacyanin

Amicyanin

## B

| | |
|---|---|
| Pseudoazurin | PGA-YLVK**C**T-P-**H**YAMG**M**IALIAVG.. |
| Rusticyanin | AGT-YYYV**C**QIPG**H**AATG**M**FGKIIVK |
| Plastocyanin | KGE-YSFY**C**S-P-**H**QGAG**M**VGKVTVN |
| Azurin | EGEQYMFF**C**TFPG**H**S-AL**M**KGTLTLK |
| Stellacyanin | VGQ-KYYI**C**GVPK**H**CDLG**Q**KVHINVT.. |
| Amicyanin | AGT-YDYH**C**T-P-**H**P-F-**M**RGKVVVE |

**Figure 5.** (A) Schematic representation of the C-terminal loop containing the Cys, HisC, and Met ligands for *Achromobacter cycloclastes* pseudoazurin,[40] *Thiobacillus ferrooxidans* rusticyanin,[41] *Populus nigra* plastocyanin,[80] *Alcaligenes xylosoxidans* azurin,[63] cucumber (*Cucumis sativus*) stellacyanin,[81] and *Paracoccus denitrificans* amicyanin.[82] (B) Sequence alignment of the same blue copper proteins. Copper ligands are colored in red. The structures (PDB files) are the same as in Table 5.

**(b) Cys Signals.** The most outstanding difference among ^{1}H NMR spectra of different BCPs concerns the $\beta$-CH$_2$ Cys proton chemical shifts, which range from 850 to 240 ppm (Table 3). We have located and assigned these resonances in Cu(II)−pseudoazurin (at 510 and 390 ppm) and Cu(II)−rusticyanin (at 300 and 240 ppm). In both cases, the chemical shifts are smaller than those of the analogous signals in plastocyanin, which possesses a classic blue site with the same ligand set (CysHis$_2$Met).

The $\beta$-Cys proton chemical shifts are dominated by the contact contribution directly related to the unpaired spin density on the S$_\gamma$(Cys) atom. The shift of each $\beta_i$-Cys proton depends on the Cu−S$_\gamma$−C$_\beta$−H$_{\beta i}$ dihedral angle through a Karplus-like equation[64] that may follow a cosine-squared or sine-squared dependence, depending on whether the mechanism of delocalization onto the Cys residue is mediated by $\pi$- or $\sigma$-type orbitals.[65] For Pc, where the stereospecific assignment of both

(61) Nar, H.; Messerschmidt, A.; Huber, R.; van de Kamp, M.; Canters, G. W. *J. Mol. Biol.* **1991**, *221*, 765−772.
(62) Murphy, L. M. M.; Strange, R. W.; Karlsson, G. B.; Lundberg, L. G.; Pascher, T.; Reinhammar, B.; Hasnain, S. S. *Biochemistry* **1993**, *32*, 1965−1975.
(63) Dodd, F. E.; Abraham, Z. H.; Eady, R. R.; Hasnain, S. S. *Acta Crystallogr. D* **2000**, *56*, 690−696.
(64) Karplus, M. *J. Am. Chem. Soc.* **1963**, *85*, 2870−2871.
(65) Bertini, I.; Capozzi, F.; Luchinat, C.; Piccioli, M.; Vila, A. J. *J. Am. Chem. Soc.* **1994**, *116*, 651−660.

$\beta$-CH$_2$ Cys protons was performed, a sine-squared dependence was proposed, suggesting a dominant $\pi$ delocalization.[22] This is consistent with the orientation of the *xy* magnetic axes in Pc that give rise to a $\pi$-type overlap between the Cu(II) d$_{x^2-y^2}$ and sulfur orbitals.[12] However, the tetragonal distortion induces a rotation of the d$_{x^2-y^2}$ orbital,[4] which is expected to give rise to a mixed $\pi$ and $\sigma$ delocalization mechanism that cannot be accurately discerned.

The average chemical shift of the $\beta$-CH$_2$ Cys protons ($\delta_{1/2}$), however, is almost independent of the Cys conformation and may be used as a reliable estimate of the electron spin density on the S$_\gamma$(Cys) atom.[31] The $\beta$-CH$_2$ Cys $\delta_{1/2}$ values (averaged from the observed shifts) are ranked in the following order: Cu(II)−azurin (825 ppm) > Cu(II)−plastocyanin (570 ppm) > Cu(II)−pseudoazurin (450 ppm) > Cu(II)−stellacyanin (415 ppm) > Cu(II)−rusticyanin (270 ppm). This indicates that the electron spin density in the S$_\gamma$(Cys) atom in pseudoazurin and rusticyanin is reduced by ∼20% and 55%, respectively, compared to that in plastocyanin. Hence, the Cu(II)−S$_\gamma$(Cys) covalence is decreased in tetragonally perturbed copper centers, in agreement with X-ray absorption data in the cucumber basic protein.[12] Interestingly, there are remarkable changes in the Cu(II)−Cys interaction in these two closely related copper sites. The X-ray structures of PsAz and Rc reveal that the Cu−S$_\gamma$(Cys) distance in Rc is 0.13 Å longer than that in PsAz (Table 5). Indeed, Rc displays the longest Cu(II)−S$_\gamma$(Cys) bond among native BCPs. It is reasonable to assume that the longer the Cu−S$_\gamma$(Cys) bond length, the smaller the electron spin density on the S$_\gamma$ atom. If this is the only geometrical factor influencing the electron delocalization, a linear relationship should be observed when plotting $1/\delta_{1/2}$ vs $r_{CuS}$ (Figure 6A). This trend holds if azurin is excluded: the Cu−S$_\gamma$(Cys) distances in azurin and pseudoazurin are similar within experimental error (Table 5), but $\delta_{1/2}$ in azurin almost doubles the value found for pseudoazurin (Table 3). Hence, this correlation cannot quantitatively account for the measured shifts of all BCPs, and other factors should be considered.

All spectroscopic and theoretical descriptions of the electronic structure of blue copper sites indicate that the unpaired electron in the oxidized state is confined to the d$_{x^2-y^2}$ orbital (orbital mixing in perturbed copper centers amounts to a d$_{z^2}$ orbital contribution <1.5% of the HOMO wave function).[12] Therefore, at a fixed Cu−S$_\gamma$(Cys) distance, the copper−sulfur overlap will depend on the displacement of the sulfur atom from the *xy* plane. As we have already pointed out, the magnetic *xy* copper axes are defined by the CuN$_{His}$N$_{His}$ plane. Hence, the largest copper−sulfur orbital overlap (either through a $\pi$ or $\sigma$ mechanism) will occur when the Cu−S$_\gamma$(Cys) bond lies in the CuN$_{His}$N$_{His}$ plane, i.e., when the angle ($\alpha$) between the CuN$_{His}$N$_{His}$ plane and the Cu−S$_\gamma$(Cys) bond is 0°. Instead, at $\alpha$ = 90°, no direct electron delocalization should be expected. The values of this angle in different BCPs are tabulated in Table 5. The copper ion in azurin is almost coplanar to the *xy* axes, while in other BCPs the copper is displaced out of this plane toward the axial ligand (Table 5). This explains the unusually large $\beta$-CH$_2$ Cys chemical shifts observed in azurin.[23] On the basis of these observations, the angular dependence could be accounted for by the following equation:

$$\delta_{1/2} = \frac{A}{r + B \, \text{tg} \, \alpha + C} \tag{4}$$

**Table 5.** Structural Parameters of Different Blue Copper Sites

| protein | copper distance (Å) to | | | | Cu out of plane (Å) | $\phi$ (deg)[a] | $\alpha$ (deg)[b] | PDB code[c] |
|---|---|---|---|---|---|---|---|---|
| | HisN N$\delta$1 | HisC N$\delta$1 | Cys S$\gamma$ | axial L | | | | |
| PsAz[d] | 1.95 | 1.92 | 2.13 | 2.71 (S$\delta$ M86) | 0.36 | 75.5 | 26.0 | 1bqk |
| Rc[e] | 2.04 | 1.89 | 2.26 | 2.89 (S$\delta$ M148) | 0.32 | 77.1 | 24.2 | 1rcy |
| Pc[f] | 1.91 | 2.06 | 2.07 | 2.82 (S$\delta$ M92) | 0.36 | 81.6 | 26.1 | 1plc |
| Az[g] | 2.04 | 1.99 | 2.14 | 3.26 (S$\delta$ M121) | 0.01 | 82.3 | −0.4 | 1dyz |
| | | | | 2.72 (O G45) | | | | |
| St[h] | 1.96 | 2.04 | 2.18 | 2.21 (O$\epsilon$ Q99) | 0.32 | 83.5 | 22.9 | 1jer |
| Am[i] | 1.95 | 2.03 | 2.11 | 2.91 (S$\delta$ M98) | 0.30 | 79.4 | 22.3 | 1aac |

[a] $\phi$ is the angle between the $N_{His}CuN_{His}$ and $S_{Cys}CuS_{Met}$ planes. [b] $\alpha$ is the angle formed by the $CuN_{His}N_{His}$ plane and the $Cu-S_\gamma(Cys)$ vector (see eq 4). [c] The PDB files used correspond to the structures with the best resolution for the corresponding oxidized BCP that exist to date in the Protein Data Bank. [d] *Achromobacter cycloclastes* pseudoazurin at 1.35 Å.[40] [e] *Thiobacillus ferrooxidans* rusticyanin at 1.90 Å.[41] [f] *Populus nigra* plastocyanin at 1.33 Å.[80] [g] *Alcaligenes xylosoxidans* azurin at 1.75 Å.[63] [h] Cucumber (*Cucumis sativus*) stellacyanin at 1.60 Å.[81] [i] *Paracoccus denitrificans* amicyanin at 1.31 Å.[82]

where $r$ is the $Cu-S\gamma(Cys)$ distance, $\alpha$ is the angle formed between the $CuN_{His}N_{His}$ plane and the $Cu-S_\gamma(Cys)$ vector, and $A$, $B$, and $C$ are parameters to be determined. For $Cu(II)-Az$, tg $\alpha = 0$ (which eliminates the angular dependence and allows us to correlate $A$ and $C$ by a simple mathematical relationship). Fitting the experimental data from the proteins in Table 5 to eq 4 yielded the following parameters: $A = 100$ ppm·Å, $B = 0.28$ Å, and $C = -2.02$ Å. The experimental $\delta_{1/2}$ and the values calculated from eq 4 show a satisfactory agreement, as shown in Figure 6B. This indicates that, notwithstanding the heuristic character of eq 4, $\delta_{1/2}$ correlates with two structural factors that affect the copper–sulfur overlap, the Cu–S bond length and the deviation of this bond from the *xy* copper axis, confirming that this parameter provides an estimate of the electron spin density on the Cys sulfur atom.

The displacement of the copper ion from the $N_{His}N_{His}S_{Cys}$ plane was initially suggested to be an indicator of a perturbed blue copper center.[66] However, plastocyanin and amicyanin present classic type 1 centers, notwithstanding the copper ion is 0.30−0.36 Å out from this plane (Table 5). Later, spectroscopic and theoretical approaches correlated the degree of tetragonal distortion to the angle subtended by the $N_{His}CuN_{His}$ and $S_{Cys}CuS_{Met}$ planes ($\phi$).[12,67] These studies revealed that the intensity ratio of the two LMCT bands at 450 and 600 nm in BCPs depends on the ratio of $\sigma$ and $\pi$ $Cu(II)-S$ overlap, i.e., on the orientation of the $Cu-S$ vector projection in the $N_{His}CuN_{His}$ plane. Here we have found that the electron spin density on the $S_\gamma(Cys)$, instead, depends on the tilting of the $Cu-S$ bond with respect to the same plane (angle $\alpha$). This clearly indicates that the degree of tetragonal distortion is not necessarily related to the strength of the $Cu(II)-S_\gamma(Cys)$ bond.

**(c) Asn41/Ser86 Signals.** In most BCPs, the amide NH proton of an Asn residue following ligand HisN forms a hydrogen bond with the $S_\gamma(Cys)$ atom.[22−24,32] Rusticyanin is an exception, since the Asn residue is replaced by a Ser.[41,43] This allows us to directly compare the hydrogen bond features of two metal sites with similar coordination geometries.

Signal G and the resonance located at −15 ppm in the $^1$H NMR spectrum of $Cu(II)-$pseudoazurin (Figure 2A) were assigned to the H$\alpha$ and peptide NH protons of Asn41, respectively (Table 1). The observed shifts are mostly due to a

contact contribution (Table 3), reflecting a net spin density onto this residue, that can be tracked to the conserved $S_\gamma(Cys)-$NH(Asn) hydrogen bond. With the exception of rusticyanin (−28.9 ppm), the contact chemical shift of this NH proton does reflect faithfully the trend observed for the $\beta$-CH$_2$ Cys $\delta_{1/2}$ values: $Cu(II)-$azurin (−39 ppm) < $Cu(II)-$plastocyanin (−28.4 ppm) < $Cu(II)-$pseudoazurin (−23.4 ppm) < $Cu(II)-$stellacyanin (−22 ppm). Instead, the position of the H$\alpha$ signal is mostly insensitive to the electron spin density on the Cys residue.[21−24]

We attempted to account for the contact shift of the Asn NH resonance by using eq 4 with the geometric parameters $A$ and $C$ and fitting the proportionality constant $A$. This yields a value of $A(NH) = -5.0$ ppm·Å. The correlation found for this NH proton is shown in Figure 6C. If we exclude rusticyanin from this plot, a linear correlation ($R^2 = 0.912$) is observed. This is an independent set of data that supports the suitability of the correlation proposed by eq 4. Hence, for BCPs containing an Asn next in sequence to HisN, the differences in the unpaired spin delocalization onto the NH of this residue depend exclusively on the electron spin density on the $S_\gamma(Cys)$.

The rusticyanin Ser86 NH proton does not follow this correlation (Figure 6C). A higher unpaired spin density is observed in this NH proton compared to that expected according to eq 4. Hence, the substitution of an Asn by a Ser in this position alters the unpaired electron density distribution in the second coordination sphere of the copper ion.

**(d) Met Signals.** Resonance M, located at 12.1 ppm, has been assigned to the $\epsilon$-CH$_3$ methyl group of Met86 in $Cu(II)-$pseudoazurin on the basis of the signal intensity and the chemical shift in the reduced form (Table 1). The estimated pseudocontact contribution for this signal is 0.8 ppm, thus revealing the existence of net electron spin density in the Met methyl group, in contrast with $Cu(II)-$plastocyanin. This may be, in principle, attributed to the shorter $Cu(II)-S_\delta(Met)$ bond in pseudoazurin (2.71 Å) compared to that in plastocyanin (2.82 Å). No Met proton resonances could be located in the $^1$H NMR spectrum of $Cu(II)-$rusticyanin outside the diamagnetic envelope. Spectra recorded in such a way to optimize detection of fast-relaxing resonances allowed us to identify an intense signal at 8.1 ppm that could correspond to the $\epsilon$-CH$_3$ Met moiety. By following the reasoning applied for the analogous resonance in pseudoazurin, the hyperfine shift in Rc might be attributed mostly to a contact contribution (Table 3) that is smaller than the $\delta_{con}$ calculated for pseudoazurin (6.0 versus 10.5 ppm, Table 3). Again, the smaller contact contribution can be attributed to

(66) Lu, Y.; LaCroix, L. B.; Lowery, M. D.; Solomon, E. I.; Bender, C. J.; Peisach, J.; Roe, J. A.; Gralla, E. B.; Valentine, J. S. *J. Am. Chem. Soc.* **1993**, *115*, 5907−5918.
(67) Pierloot, K.; De Kerpel, J. A. O.; Ryde, U.; Olsson, M. H.; Roos, B. O. *J. Am. Chem. Soc.* **1998**, *120*, 13156−13166.
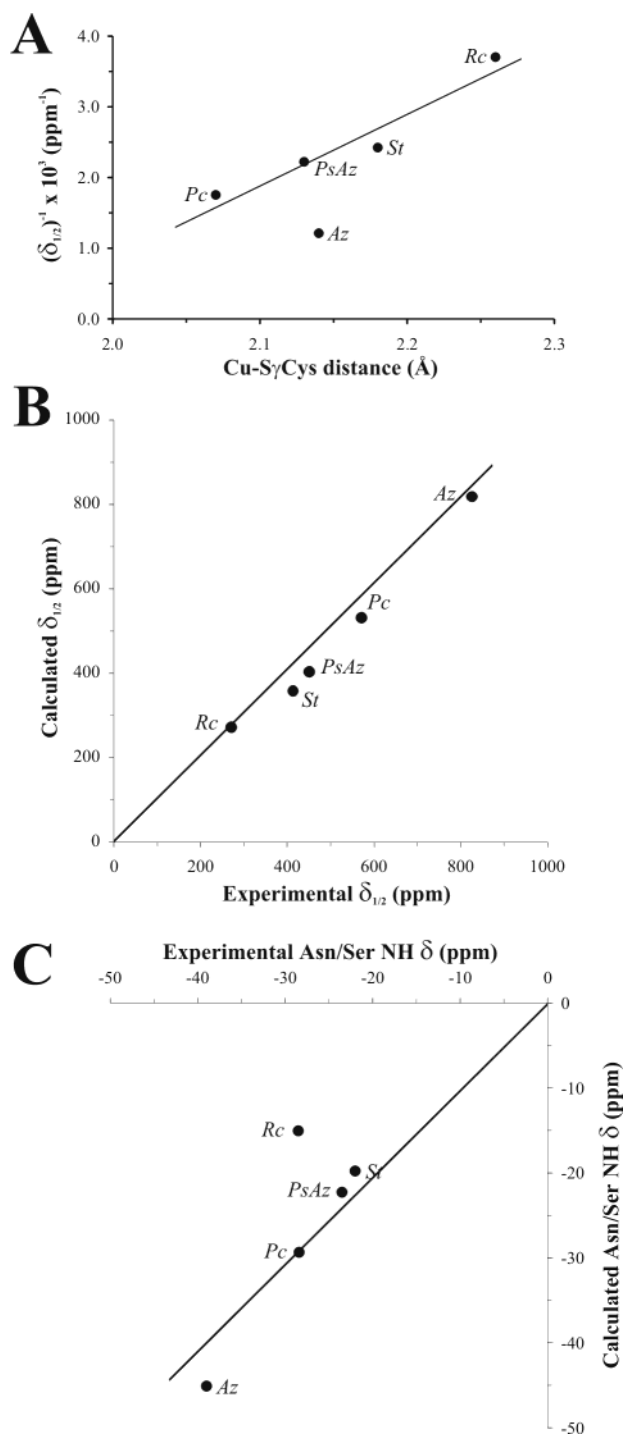
**Figure 6.** (A) Plot of the reciprocal $\delta_{1/2}$ (see text) for the $\beta$-CH$_2$ Cys protons as a function of the Cu–S$_\gamma$(Cys) distance. Errors in $r$(Cu–S) distances are < 0.04 Å. (B) Plot of the inverse of the calculated $\delta_{1/2}$ for $\beta$-CH$_2$ Cys versus the observed values according to eq 4. (C) Plot of the reciprocal calculated contact chemical shifts for the Asn/Ser86 NH versus the experimental values according to eq 4. Parameters $A$, $B$, and $C$ are given in the text.

the longer Cu(II)–S$_\delta$(Met) distance in rusticyanin than that in pseudoazurin (Table 5).

The $\gamma$-CH$_2$ Met resonances have been identified in the spectra of Cu(II)–plastocyanin (at 23.5 and 13.0 ppm)[22] and Cu(II)–amicyanin (11.1 and 12 ppm)[21] and are absent in the spectra of Cu(II)–pseudoazurin and Cu(II)–rusticyanin. These differences can be attributed to the observation that the Met side chain

adopts a trans conformation in classic blue sites and a gauche conformation in tetragonally distorted sites.[68] These distinct conformations clearly lead to different electron delocalization patterns in the axial Met. Hence, even if NMR data are limited for this residue, they are indicative of the Met side chain conformation.

**Electronic Structure and Molecular Frame.** This NMR study reveals common features of the electronic structure of Cu(II)–pseudoazurin and Cu(II)–rusticyanin. The electron spin density on the Cys ligand is reduced, while the electron delocalization pattern of the axial (Met) ligand is different when compared to that of Pc, reflecting the different orientation of the Met residue. The decrease of the $\beta$-CH$_2$ Cys $\delta_{1/2}$ in pseudoazurin (with a Cu(II)–S$_\delta$(Met) distance of 2.71 Å) with respect to plastocyanin is almost as large as that induced in stellacyanin by the presence of an axial Gln ligand at 2.2 Å. The effect on rusticyanin is even more drastic and can be attributed to the longer Cu(II)–S$_\gamma$(Cys) bond (note that the longer Cu–Cys bond is not imposed by the axial Met ligand interaction; see below).

This work also reveals subtle differences between PsAz and Rc that are not evident from other spectroscopies. The spectral ratio of the LMCT bands ($\epsilon_{450}/\epsilon_{600}$) equals 0.41 in PsAz and 0.47 in Rc, and the EPR patterns are very similar. This is in agreement with the close values of the $\phi$ angles in both proteins (Table 5), which predicts a similar degree of tetragonal distortion. Instead, NMR data reveal that strikingly different Cu(II)–Cys bonding features can be monitored in PsAz and Rc. This implies that similar tetragonal distortions can be induced by different metal–ligand interactions and that the geometric distortion of the metal site, and not exclusively the copper–axial ligand interaction, is able to affect the electronic structure of type 1 sites. Finally, we conclude that the structural features that govern the electron spin density on each copper ligand differ from those giving rise to the tetragonal distortion.

The crystal structures indicate that, although the Cu(II)–S$_\delta$(Met) in rusticyanin is slightly longer when compared to those in pseudoazurin and plastocyanin (see Table 5), the Cu(II)–S$_\gamma$(Cys) bond is also long. It can also be concluded that the strength of Cu(II)–S$_\gamma$(Cys) and Cu(II)–S$_\delta$(Met) interactions may be independently modulated in tetragonally distorted type 1 sites. This would agree with the data from the crystallographic structures of blue and green NiRs, where no observable differences in the Cu(II)–S$_\delta$(Met) distances have been found; in fact, only a significant difference in the HisC–Cu–Met angle is observed between the blue and perturbed (i.e., green) sites.[15]

This observation is in conflict with the trend observed in the azurin–plastocyanin–stellacyanin series, in which a shorter copper–axial ligand bond was shown to give rise to a decreased Cu(II)–S$_\gamma$(Cys) covalence.[23] However, this correlation may hold for classic and tetrahedrally perturbed sites, in which the axial perturbation displaces the copper ion out from the equatorial plane, with no significant angular distortions.

The Cys and Met ligands in all cupredoxins are located near the $\beta$-strands in the loop containing the exposed HisC ligand (Figure 5).[1] These residues exhibit a low backbone mobility, as revealed by NMR relaxation studies in different cupredoxins.[24,69,70,71] The $\beta$-sheets could then fix the Cys and

(68) Guss, J. M.; Merritt, E. A.; Phizackerley, R. P.; Freeman, H. C. *J. Mol. Biol.* **1996**, *262*, 686–705.

Met orientations and distances to the copper ion. This is in agreement with an elegant "loop-mutagenesis" study, in which several loops imitating different BCP ligand loops were inserted in amicyanin.[59] Resonance Raman spectra of these mutants revealed that the Cu–$S_\gamma$(Cys) interactions were the same for all the chimeric proteins; i.e., cysteine (as methionine)–metal relative orientations and interactions were governed by their position in their $\beta$-strands, not in the mutant loops.[59] Moreover, an amicyanin mutant with the PsAz loop exhibited a perturbed type 1 site, but the mutant did not reproduce the spectral features of pseudoazurin. The present NMR data are fully consistent with the conclusions from the loop mutagenesis study. Inspection of Figure 5 confirms this view, since pseudoazurin and plastocyanin possess a similar loop spacing and loop conformation, but different electronic structures due to the relative orientation of the Cys and Met ligands. Instead, pseudoazurin and rusticyanin display a similar tetragonal distortion, notwithstanding the differences in the loop conformation.

HisC is in the middle of the mentioned loop (Figure 5), in such a way that this ligand could adopt different conformations in the copper site. However, the fairly constant hyperfine shifts observed for this histidine in all BCPs (Table 3) indicate that the orientation of the copper ligand HisC is governed by the Cu–$N_{\delta1}$(His) interaction. Therefore, an intricate ensemble of interactions (mostly determined by the $\beta$-barrel fold and not by the loop) contributes to determine the geometric and electronic structure of tetragonally distorted sites.

**Implication in BCPs' Redox Potentials.** Factors governing the thermodynamics of the redox process in BCPs have been studied recently by Sola and co-workers.[72–74] Enthalpic effects, mainly due to metal–ligand interactions and metal site electrostatics, mostly govern redox potentials, even if entropic contributions are not negligible at all.[73] NMR allows us to evaluate the different metal–ligand interactions, thus directly providing information on the enthalpic term.

Rusticyanin displays the highest redox potential among BCPs (680 mV),[36,39,46] which has been partially attributed to the highly hydrophobic environment of the metal site[36,41,43,44] and the substitution of Ser for Asn adjacent to the HisN ligand.[46] The side-chain oxygen of Ser86 in the structure of the native protein[75] (and also in M148Leu[76] and M148Gln[77] structures) forms two hydrogen bonds. The first is a tight [2.73 Å (2.79, 2.98 Å)] bond to the backbone nitrogen of Gln139, while the second H-bond links to the side-chain oxygen of Asp88 [2.9 Å (2.72,2.97 Å)]. Additionally, the backbone nitrogen of Ser86 provides a hydrogen bond to the sulfur of the copper ligand Cys138. This H-bond interaction is expected to directly affect the copper redox potential. Substitution of Ser86 by site-directed

mutagenesis results in a lowered redox potential, in agreement with this proposal.[46] Figure 6C gives evidence that the unpaired spin density residing on this NH exhibits a larger contact shift than that expected from the trend displayed by other BCPs, suggesting a less negative character in the sulfur atom. This feature clearly destabilizes the oxidized species in Rc, raising the redox potential. Our results thus allow us to describe the effects induced by Ser86 on the electronic structure of the copper site in rusticyanin.

The $\beta$-CH$_2$ Cys $\delta_{1/2}$ value in Rc is the lowest in the BCP series (Figure 6B). However, no correlation between the redox potential and the chemical shifts in these BCPs has been found. The copper–$S_\delta$(Met) interaction may also contribute to the redox potential in BCPs.[11,78] However, the contribution of the Cu–$S_\delta$(Met) bond to the redox potential in BCPs is difficult to estimate quantitatively. It is interesting to note that azurin shows a higher redox potential in the unfolded state than in the folded form,[10,11] notwithstanding the higher degree of solvent exposure of the metal site. NMR studies have demonstrated that the axial Met is detached from the metal ion in partially unfolded azurin.[79] On the basis of these considerations, a weaker Cu–$S_\delta$(Met) interaction in rusticyanin could further contribute to destabilize the Cu(II) state, thus raising the redox potential.[9]

## Conclusions

Here we have learned the following: (1) NMR provides an accurate description of the electron spin density around the copper(II) ion in BCPs. This technique reveals subtle differences that are not evident in optical nor in EPR spectra but correlate with results from high-resolution crystal structures. (2) The electron spin density in the Cys ligands in tetragonally distorted BCPs is decreased compared to that in classic type 1 sites, but this is not necessarily related to a stronger interaction with the axial ligand. (3) The Cu–Cys and the Cu–Met interactions may be independently tuned by the protein folding around the metal site in tetragonally distorted blue copper sites. (4) The $\beta$-CH$_2$ Cys $\delta_{1/2}$ and the $\delta_{con}$ of the NH Asn reflect the electron spin density in the $S_\gamma$(Cys) atom, which can be accounted for by geometric features of the metal site (the Cu–$S_\gamma$(Cys) distance and the angle between the CuN$_{His}$N$_{His}$ plane and the Cu–$S_\gamma$(Cys) vector) that do not correlate with the degree of tetragonal distortion. The proposed correlation might have predictive value. (5) The electron spin density in $S_\gamma$(Cys) atom in rusticyanin is substantially reduced, notwithstanding the long Cu(II)–S(Met) bond. This might be due to the distinct hydrogen-bonding interaction with Ser86 NH, in contrast to the general trend followed by other BCPs.

(69) Bertini, I.; Ciurli, S.; Dikiy, A.; Fernandez, C. O.; Luchinat, C.; Safarov, N.; Shumilin, S.; Vila, A. J. *J. Am. Chem. Soc.* **2001**, *123*, 2405–2413.
(70) Kalverda, A. P.; Ubbink, M.; Gilardi, G.; Wijmenga, S. S.; Crawford, A.; Jeuken, L. J.; Canters, G. W. *Biochemistry* **1999**, *38*, 12690–12697.
(71) Reader, J. S.; Van Nuland, N. A.; Thompson, G. S.; Ferguson, S. J.; Dobson, C. M.; Radford, S. E. *Protein Sci.* **2001**, *10*, 1216–1224.
(72) Battistuzzi, G.; Borsari, M.; Loschi, L.; Menziani, M. C.; De Rienzo, F.; Sola, M. *Biochemistry* **2001**, *40*, 6422–6430.
(73) Battistuzzi, G.; Borsari, M.; Loschi, L.; Righi, F.; Sola, M. *J. Am. Chem. Soc.* **1999**, *121*, 501–506.
(74) Battistuzzi, G.; Borsari, M.; Canters, G. W.; de Waal, E. C.; Loschi, L.; Warmerdam, G. C. M.; Sola, M. *Biochemistry* **2001**, *40*, 6707–6712.
(75) Harvey, I.; Hao, Q.; Duke, E. M.; Ingledew, W. J.; Hasnain, S. S. *Acta Crystallogr. D* **1998**, *54*, 629–635.
(76) Kanbi, L. D.; Antonyuk, S.; Hough, M. A.; Hall, J. F.; Dodd, F. E.; Hasnain, S. S. *J. Mol. Biol.* **2002**, *320*, 263–275.
(77) Hough, M. A.; Hall, J. F.; Kanbi, L. D.; Hasnain, S. S. *Acta Crystallogr. D* **2001**, *57*, 355–360.

(78) Solomon, E. I.; Penfield, K. W.; Gewirth, A. A.; Lowery, M. D.; Shadle, S. E.; Guckert, G. A.; LaCroix, L. B. *Inorg. Chim. Acta* **1996**, *243*, 67–78.
(79) Romero, C.; Moratal, J. M.; Donaire, A. *FEBS Lett.* **1998**, *440*, 93–98.
(80) Guss, J. M.; Bartunik, H. D.; Freeman, H. C. *Acta Crystallogr. B* **1992**, *48*, 790–811.
(81) Hart, P. J.; Nersissian, A. M.; Herrmann, R. G.; Nalbandyan, R. M.; Valentine, J. S.; Eisenberg, D. *Protein Sci.* **1996**, *5*, 2175–2183.
(82) Cunane, L. M.; Chen, Z. W.; Durley, R. C. E.; Mathews, F. S. *Acta Crystallogr. D* **1996**, *52*, 676–686.

JA0267019